Formation of Na containing complex molecules in the gas phase in dense molecular clouds: Quantum study of the Na + +H 2 and Na + +D 2 radiative association step

Daria Burdakova, Gunnar Nyman, Thierry Stoecklin

Formation of Na containing complex molecules in the gas phase in dense molecular clouds: Quantum study of the $Na^+ + H_2$ and $Na^+ + D_2$ radiative association step

Daria Burdakova,[1] Gunnar Nyman,[1] Thierry Stoecklin ,[2]★
[1] *Department of Chemistry and Molecular Biology, University of Gothenburg, 41296 Gothenburg, Sweden*
[2] *Université de Bordeaux, ISM, UMR 5255, 33405, Talence, France*

Accepted XXX. Received YYY; in original form ZZZ

ABSTRACT
The $Na^+ - H_2$ radiative association (RA) is the first and limiting step in the models of formation of NaH in the gas phase. Also the accurate evaluation of the RA rate is required to be included in chemical models of dense molecular clouds. In this work a quantum study of the formation of the $Na^+ - H_2$ and $Na^+ - D_2$ complexes by radiative association is presented. We use a 3D potential energy surface published recently and a quantum dynamical method based on the driven equation formalism. The values obtained for the radiative association rates are compared with previous evaluations based on approximate methods and the possible role played by these two processes in the gas phase chemistry of dense molecular clouds is discussed.

Key words: astrochemistry – radiative association– molecular data – molecular processes – scattering – ISM: molecules.

1 INTRODUCTION

Metals were for a long time considered not to play an important role in the gas-phase chemical processes of interstellar clouds. This assumption was motivated by the common belief that the metals mostly accumulated on dust-grain surfaces (Petrie & Dunbar 2000). Also, metals were only thought to participate in two types of processes: radiative recombination with free electrons and charge transfer reactions with neutrals. While the former is slow, the latter is improbable as the ionization energies of neutrals are often too high to allow charge transfer. The last motivation for neglecting metals in interstellar cloud reactions was that early studies involving Na^+ and Mg^+ reacting with some neutrals gave very low reaction rates.

Now the assumption that metals are unimportant in gas phase chemistry is for debate, mostly because several molecules containing metals like NaCl, AlF or KCl were observed in the envelope of IRC+1026 (Petrie & Dunbar 2000). NaH was also searched for by Plambeck & Erickson (1982) but unsuccessfully up to now. The authors of this later study conclude that the observed upper limit of the fractional abundance of NaH in Orion is at least two orders of magnitude smaller than what would be predicted if NaH were formed efficiently on grains. It is furthermore consistent with the upper limit expected from ion-molecule chemistry when using the estimation of $Na^+ - H_2$ RA by Smith et al. (1983) which was available at that time. In any case, the occurrence of association reactions of the abundant metal ions with interstellar molecules may have important implications for cloud chemical evolution, even if these reactions do not lead to significant abundances of any metal-containing molecules.

The gas phase mechanism of formation of such molecules within the Smith et al. (1983) model involves two steps: first the radiative association of the cationic form of the metal M^+ with H_2:

$$M^+ + H_2 \longrightarrow M^+ - H_2 + h\nu$$

followed by the following channel of the dissociative recombination process with electron:

$$M^+ - H_2 + e^- \longrightarrow MH + H^+$$

This mode of depletion of M^+ is in competition with the radiative recombination with an electron. In the case of Na^+ the rate coefficient of this process at 20 K was estimated by Prasad & Huntress (1980) to be $k_{RR}^{e^-} = 1.7 \times 10^{-11} \mathrm{cm^3 s^{-1}}$.

Knowing the fractional abundance f_e of electrons relative to H_2 one can deduce the minimum value of the RA rate coefficient k_{RA} with H_2 which would make this process important for the chemistry of the cloud:

$k_{RA}^{H_2} \geqslant\geqslant k_{RR}^{e^-} * fe$

Two evaluations of the $Na^+ - H_2$ RA rate coefficients were obtained using approximate methods. Herbst and

★ E-mail: thierry.stoecklin@u-bordeaux.fr

coworkers obtained the first evaluation of the RA rate coefficient in 1983 (Smith et al. 1983). They found a rate coefficient almost independent of temperature and equal to $4 \cdot 10^{-19}$cm^{3}molecule^{-1}s^{-1}. This would lead to a fractional abundance of electron relative to H_2 lower than 2.6×10^{-8} which is close to its usual estimate in dense molecular clouds. These authors then concluded that the $Na^+ - H_2$ RA process could play a role in the chemistry of dense molecular clouds and needed to be included in the chemical models of dense molecular clouds. More recently, Petrie & Dunbar (2000) performed calculations based on transition state theory and obtained a rate varying with temperature. The value at 30 K is $8.7 \cdot 10^{-23}$cm^{3}molecule^{-1}s^{-1} which is four orders of magnitude smaller than the evaluation by Herbst and coworkers. These later results would exclude the $Na^+ - H_2$ RA process from the chemistry of dense molecular clouds.

This difference motivates the need for a more accurate study based on the close coupling approach in order to determine the role of this process in the chemistry of intermolecular clouds. We present a quantum study of the formation of the $Na^+ - H_2$ and $Na^+ - D_2$ complexes by radiative association (RA).

Recent investigations of the $Na^+ - H_2$ and $Na^+ - D_2$ complexes were performed by Poad et al. (2008, 2011). They performed experimental measurements and *ab initio* calculations of the rotationally resolved rovibrational spectrum of these two complexes. In their studies very good agreement between theory and experiment was obtained, which demonstrated the high accuracy of their potential energy surface (PES). In the present work we use the 3D PES and dipole moment surfaces calculated by those authors to study the radiative association to form these two complexes. Close Coupling (CC) radiative association calculations are routinely performed for diatomics like CH, CH^+, NH, NO, CN, CO, C_2, OH (Julienne & Krauss 1973; Nyman et al. 2015), while available calculations for triatomic systems are limited to the five systems: $H_2^+ + He$ (Mrugala et al. 2003), $H^- + H_2$ (Ayouz et al. 2011), $H^- + N_2$ (Stoecklin et al. 2013) and very recently $H + CO$ (Stoecklin et al. 2018b) and $H^- + CO$ (Stoecklin et al. 2018a) . The methods developed in the last three of the above mentioned studies are used in the present work as well.

The manuscript is organized as follows: In section II we briefly describe the main features of both the PES and the dipole moment surface calculated by Poad et al. (2008, 2011) and we summarize the main steps of the method used to calculate the RA rate coefficient. In section III we present and discuss the results. The possible importance of the RA process for these two systems in the chemistry of molecular clouds is discussed in section IV.

2 METHODS

Throughout this article the same Jacobi coordinates are used to describe the initial scattering state and the final bound state. These coordinates are illustrated in figure 1, where r is the distance between the atoms in the diatomic molecule (H_2 or D_2). R is the distance between the center of mass of the diatomic molecule and the sodium atom and θ is the angle between R and r.

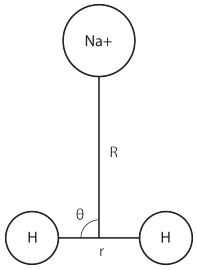

Figure 1. Jacobi coordinates for the $Na^+ + H_2$ system.

2.1 Potential energy surface and dipole moment

We use the 3D potential energy surface and dipole moment surface calculated by Poad et al. (2008, 2011). In summary both are based on a large grid of 1850 spin-restricted coupled cluster calculations (RCCSDT) using a cc-pVQZ and an aug-cc-pVQZ basis set for the sodium and the hydrogen atoms respectively. The three lowest vibrational levels of H_2 are accurately described on this grid where the vibrational coordinate r ranges from 1 to 3 Bohr in steps of 0.2 Bohr. The intermolecular coordinate R varies from 3 up to 40 Bohr in order for the long range potential to be well represented.

Poad et al. (2008) obtained an analytical representation of the 3D PES by using the Reproducing Kernel Hilbert Space method (RKHS) by Hollebeek et al. (1999). Outside the upper limit of the *ab initio* grid the analytical RKHS long range potential varies as $1/R^4$, as expected for a charge induced dipole potential. The minimum geometry of the complex is T shaped and its energy is 1184 cm^{-1} below the zero point level of the reactants. The rovibrational calculations performed by Poad et al. (2008) predict that the ground state of the $Na^+ - pH_2$ (para hydrogen) complex lies $D_0 = 842\,\mathrm{cm}^{-1}$ below the $Na^+ - H_2(j = 0)$ limit and that the ground state of the $Na^+ - oH_2$ (ortho hydrogen) complex lies 888 cm^{-1} below the $Na^+ - H_2(j = 1)$ limit. The corresponding calculated binding energies of Poad et al. (2011) for the $Na^+ - D_2$ complex are found to be 923 cm^{-1} and $949\,\mathrm{cm}^{-1}$ respectively for the ortho and para species. Due to its slightly lower vibrational zero point energy, $Na^+ - oD_2$ is then bound 81 cm^{-1} more strongly than $Na^+ - pH_2$.

From the above it is possible to conclude that the intermolecular potential is not strong enough to vibrationally excite H_2 or D_2. The equilibrium r distance in the complex is furthermore very close to its free diatom value, supporting the assumption that vibrational coupling is not very strong and suggesting that the rigid rotor approximation could be considered for performing both the Bound states and the dynamics calculations. We choose an intermediate solution by including in both types of calculations only the lowest vibrational state of the diatom and integrating over the vibrational coordinate. The associated 3D dipole moment function calculated by Poad et al. (2008, 2011) is a linear combination of Legendre polynomials and of powers of the intermolecular and vibrational coordinates. They found that accordingly to the model we used for the N_2H^- and HCO^-systems, the intermolecular component of the dipole moment varies like R and that the other components are negligible.

2.2 Bound states and Dynamics

The dynamics calculation are performed using the method that we developed in previous work dedicated to the N_2+H^- radiative association (Stoecklin et al. 2013). A brief account of this procedure is given below. The interested reader may find more details in our original work (Stoecklin et al. 2013).

The method that we used is based on the driven equation formalism and is an adaptation of the method developed for photo-dissociation by Band et al. (1981), Balint-Kurti & Shapiro (1981) and Heather & Light (1983). The driven equation method connects the initial and the final wave functions of the colliding system through the matter-radiation interaction operator. We use the same Jacobi coordinates (R,r,θ) (see figure 1) and coupled angular basis sets for the expansion of the initial and final nuclear wave functions in the space fixed frame:

$$Y_{jl}^{JM}(\hat{r},\hat{R}) = \sum_{m_j,m_l} \langle jm_j lm_l \| JM\rangle y_j^{m_j}(\hat{r}) y_l^{m_l}(\hat{R}) \tag{1}$$

where j, l and J are respectively the quantum numbers associated with the rotational angular momentum of the diatom $\vec{j}$, the orbital angular momentum $\vec{l}$ and the total angular momentum $\vec{J} = \vec{j} + \vec{l}$. In this basis set the initial $\Psi_i(R,r,\theta)$ and final $\Psi_f^{\alpha}(R,r,\theta)$ wave functions of the system are respectively written like:

$$\Psi_i^{JM}(R,r,\theta) = \frac{1}{Rr} \sum_{v,j,l} \chi_{v,j,l}^{JM}(R)\varphi_{vj}(r) Y_{jl}^{JM}(\hat{R},\hat{r}) \tag{2}$$

$$\Psi_f^{\alpha J'M'}(R,r,\theta) = \frac{1}{Rr} \sum_{v',j',l'} \omega_{v',j',l'}^{\alpha J'M'}(R)\varphi_{v'j'}(r) Y_{j'l'}^{J'M'}(\hat{R},\hat{r}) \tag{3}$$

In this expression α denotes bound states, $\chi_{v,j,l}^{JM}(R)$ and $\omega_{v',j',l'}^{\alpha J'M'}(R)$ are the radial parts in R of the initial and final wave functions, while $\varphi_{vj}(r)$ and $\varphi_{v'j'}(r)$ are the corresponding radial parts in r. We furthermore use the hydrogen exchange symmetry of the system and make separate calculations for the two spin isomers of H_2 and D_2.

2.2.1 Bound state calculations

In our previous work dedicated to N_2H^-(Lique et al. 2012; Stoecklin et al. 2013) we used an adaptation of the CC method proposed by (Hutson 1994), which is also detailed in a previous study dedicated to Ar – NO^+ (Halvick et al. 2011). In this study we use the same variational approach (Ajili et al. 2016) as in our work dedicated to HCO^- (Stoecklin et al. 2018a).

The computations are performed by using the analytical expansion (1) for the angular basis set. A Chebyshev DVR grid of 400 points in the range [3.0,80.0] a_0 is used to describe the R radial part of the wave function and 18 Gauss-Hermite points in the range [0.725,2.09] a_0 are used for the vibrational coordinate r, along with 10 rotational basis functions for each spin isomer of H_2 and D_2.

2.2.2 Dynamics

The radial part of the total wave function describing the system before and after radiative association is a solution of the following equation:

$$\left[\frac{d^2}{dR^2} - \frac{l(l+1)}{R^2} + k_{vj}^2(E) - U_{vjl}^{v'j'l'}(R)\right]\chi_{vjl}^{v'j'l'}(R) = \lambda_{vjlJM}^{\alpha J'M'}(R) \tag{4}$$

where k_{vj} are channel wave vectors and $U_{vjl}^{v'j'l'}$ are the matrix elements of the intermolecular potential. The term appearing on the right hand side of the close coupled equations, $\lambda_{vjlJM}^{\alpha J'M'}(R)$, is called the driving term. It is real and results from the dipolar coupling of the initial scattering and final bound states within the dipolar approximation.

$$\lambda_{vjlJM}^{\alpha J'M'}(R) = -2\mu_{Na^+-H_2} \int d\hat{R}d\hat{r}dr\varphi_{vj}(r)[Y_{jl}^{JM}(\hat{r},\hat{R})]^* \times \mu(\vec{R},\vec{r})\Psi_f^{\alpha,J',M'}(R,r,\theta) \tag{5}$$

For a charged atom interacting with a neutral diatom, the dipole moment of the system can safely be assumed to lie along the intermolecular axis (R-direction). This is indeed confirmed by the *ab initio* dipole moment calculated by Poad et al. (2008, 2011). If we further neglect the diatomic vibrational dependence of the dipole and take it to be proportional to R, then equation 5 can be simplified to:

$$\lambda_{vjlJM}^{\alpha J'M'}(R) = \frac{-2\mu_{Na^+-H_2}^2}{m_{Na^+}}\delta_{v,v'} \sum_{j',l'} \Gamma_{vjlJ}^{vj'l'J'} R\omega_{vj'l'}^{\alpha,J',M'}(R) \tag{6}$$

where

$$\Gamma_{vjlJ}^{vj'l'J'} = \delta_{jj'}[(2J+1)(2J'+1)(2l+1)(2l'+1)]^{\frac{1}{2}} \times (-)^{(2J+l+l'+1)} \sum_{j',l'} \begin{pmatrix} l & 1 & l' \\ 0 & 0 & 0 \end{pmatrix} \begin{Bmatrix} l & J & j \\ J' & l' & 1 \end{Bmatrix} \tag{7}$$

The scattering wave function is propagated using a Magnus propagator from the classically forbidden region out to the asymptotic region. In the asymptotic region the boundary condition of an incoming plane wave is applied as detailed in our previous work. The radiative association cross section for a given initial rovibrational state (v,j) of H_2 is then obtained from the following expression:

$$\sigma_{v,j}(E) = \frac{8\pi^2\omega_\alpha^3}{3k_{vj}^2C^3} \sum_{J,J',\alpha} \left[M_{v,j,J}^{\alpha,J'}(E)\right]^2 \tag{8}$$

where a summation is performed over all the possible values of the initial and final total angular momenta and over the possible bound states. ω_α is the frequency of the corresponding emitted photon and $M_{v,j,J}^{\alpha,J'}(E)$ are state selected driving terms integrated over R as detailed in our previous work (Stoecklin et al. 2013).

3 RESULTS

A 3D contour plot in Jacobi coordinates of the PES developed by Poad et al. (2008) is presented in figure 3 where the

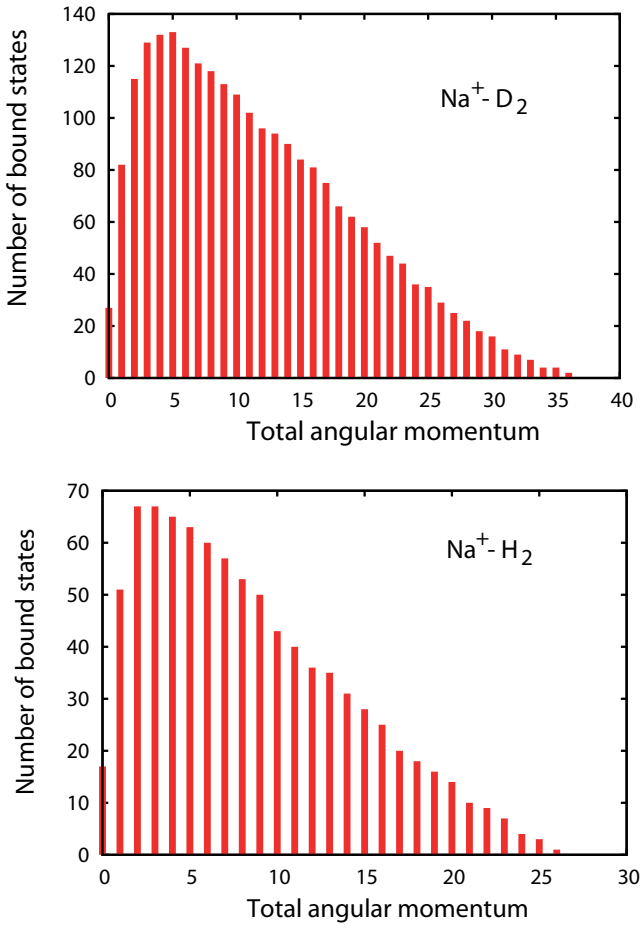

Figure 2. Comparison between the number of bound states of the $Na^+ - H_2$ and $Na^+ - D_2$ complexes as a function of the total angular momentum of the system.

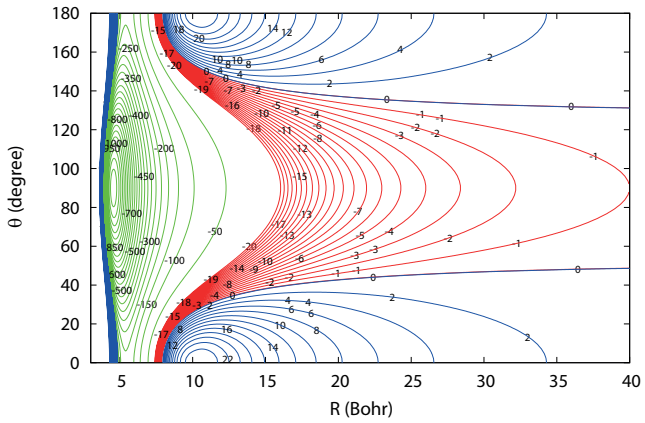

Figure 3. Potential energy surface for $Na^+ + H_2$ obtained by Poad et al.

diatomic bond length r is fixed at 1.41 Bohr. The strong long range potential as well as the T shaped equilibrium geometry of the complex (for R=4.7 Bohr) appear both clearly on this figure.

As usual for complexes including homonuclear molecules, the two nuclear spin isomers of H_2 and D_2 were treated separately. We took into account the states with positive energy that are located above the $j = 0$ state of H_2 or D_2 but are bound because they have no open channels for rotational predissociation. These are all the states with odd parity which are below the $j = 1$ threshold as well as the states with even j parity below the $j = 2$ threshold. This results in the need to include 457 para and 432 ortho bound states in the calculations of the RA of the Na^+-H_2 complex. For the Na^+-D_2 complex even more bound states need to be included - 1161 para and 1214 ortho states.

The rotational basis sets used for the initial and final states of the systems are each made up of ten rotational states with j ranging from 0 to 18 for para H_2 and ortho D_2 while j is taken to vary from 1 to 19 for ortho H_2 and para D_2. With these basis sets the highest values of the total angular momentum J giving bound states are 26 for $Na^+ - pH_2$ and 25 for $Na^+ - oH_2$ and 36 for both $Na^+ - pD_2$ and $Na^+ - oD_2$. These results are illustrated in figure 2 where the number of bound states of the $Na^+ - H_2$ and $Na^+ - D_2$ complexes as a function of the total angular momentum J are compared. As expected for such ionic systems, the density of bound states increases near the dissociation threshold of the complex (Munro et al. 2005) as a result of the strength of the long range part of the interaction potential. Also, one could be tempted to expect these states to give an important contribution to the RA cross section and to give a special attention to their accurate determination. However, the driving term components associated with these states can be large only at very low collision energy. This means that the corresponding frequency ω_α of the emitted photon is also very small as is the associated RA cross section component which is proportional to ω_α^3. This discussion is illustrated in figure 4 where is presented the variation of the driving terms associated with two different bound states as a function of the intermolecular coordinate for J=0 and a collision energy of 1 cm^{-1}.

It can be seen that the driving term gives a very intuitive picture of the RA process. Clearly, the lower bound states which are localized in a narrower intermolecular distance interval give a localized driving term while the most excited bound states extend over a large intermolecular range and give rise to an extended domain of the driving term. As the cross section is directly proportional to the square of the integral of the driving term at a given collision energy, some of the bound states give larger contributions to the cross sections.

The variation of the $Na^+ + H_2$ RA cross sections as a function of collision energy are shown for the para and ortho species of H_2 for various initial rotational states of the diatomic fragment respectively in the lower and upper panels of figure 5. It can be seen in this figure that the RA cross section of ortho H_2 with Na^+ decrease when the rotational excitation of H_2 increases while for para H_2 the j=2 gives larger RA cross sections than j=0 and j=4.

The dependence of the $Na^+ + D_2$ cross sections on the collision energy is depicted in figure 6. Comparing these results with the ones shown in figure 5, it can be observed that both $Na^+ + H_2$ and $Na^+ + D_2$ exhibit the same behavior when it comes to the difference in magnitude of cross sections corresponding to different values of j with also the $j = 2$ cross section lying higher than the $j = 0$ and $j = 4$

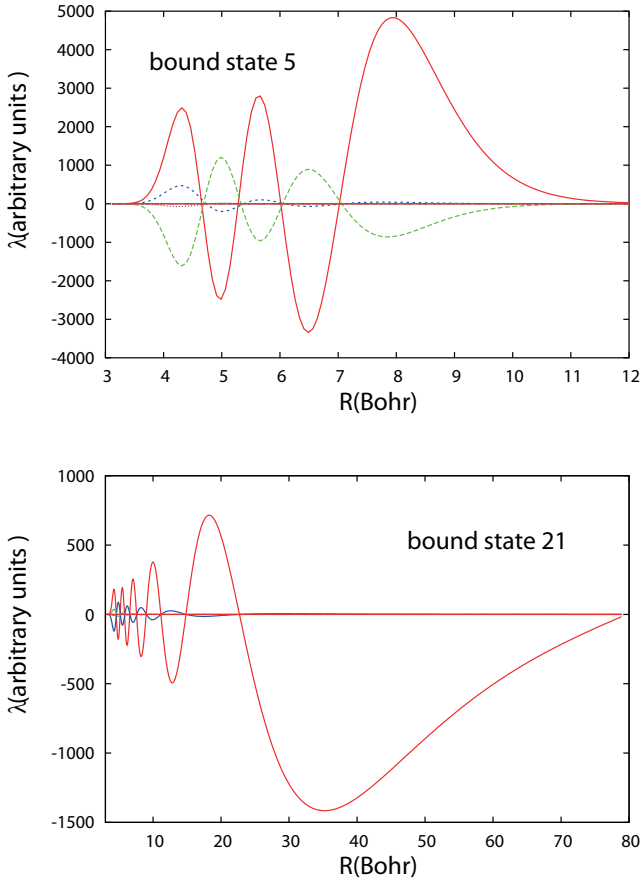

Figure 4. Variation of the driving term associated with two different bound states as a function of the intermolecular coordinate for J=0 and a collision energy of 1 cm^{-1}.

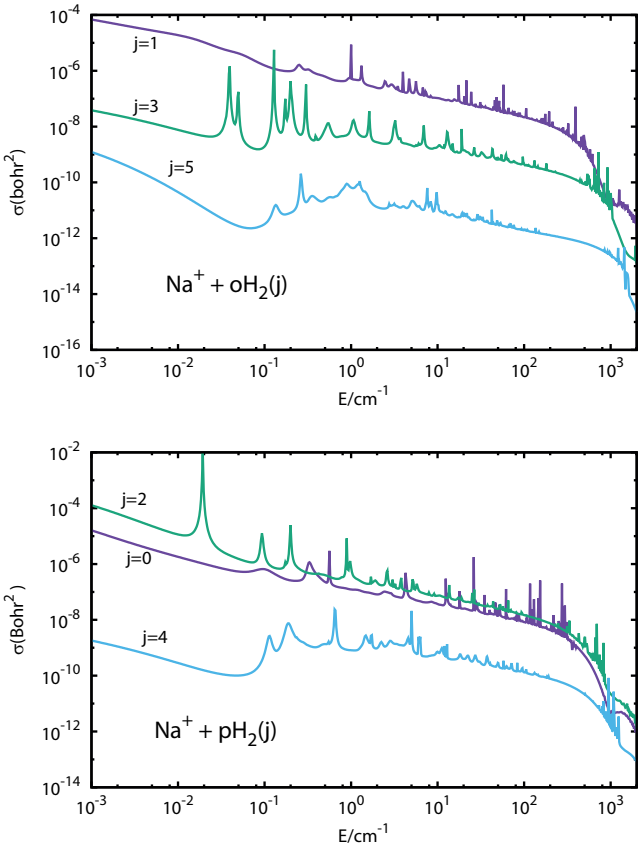

Figure 5. Dependence of the $Na^+ + H_2(v = 0, j)$ RA cross section as a function of rotational excitation illustrated for three values of the rotational quantum number of each of the two spin isomers of H_2 : The upper panel shows the results for the j = 1, 3, 5 states of ortho H_2 while the lower panel shows those for the j = 0, 2, 4 states of para H_2.

cross sections. Mostly the $Na^+ + D_2$ cross sections are larger than the $Na^+ + H_2$ ones, which at least partly is due to the larger number of bound states for the $Na^+ - D_2$ complex.

In figures 7 and 8 j-resolved rate coefficients are shown as a function of temperature for $Na^+ + H_2$ and $Na^+ + D_2$, respectively. The results of Boltzmann averaging are also shown in these two figures for each spin isomer. The large cross section of the j=2 state has a significantly larger effect on the Boltzmann averaged rate coefficients in the case of $Na^+ + D_2$ than for $Na^+ + H_2$ since the j = 2 level of D_2 is thermally more accessible than it is for H_2 .

Figure 9 summarizes the rate coefficients for the $Na^+ + H_2$, lower panel, and $Na^+ + D_2$, upper panel, reactions. The panels show thermal rate coefficients obtained separately for ortho states and for para states and also the Boltzmann weighted average of these. When combining the o-D_2 and p-D_2 rate coefficients a ratio of 2:1, obtained from spin statistics is included. The same was done for $Na^+ + H_2$ using ratio of 3:1 between the ortho and para states.

Comparing the total rate coefficients of $Na^+ + D_2$ and $Na^+ + H_2$ we can see that both curves are smooth with a bump at higher temperatures after which the rates decrease monotonously. The $Na^+ + D_2$ complex shows a much bigger bump than the $Na^+ + H_2$ complex due to the thermal accessibility of the j = 2 state. The total rate coefficient is mostly larger for $Na^+ + D_2$ than for $Na^+ + H_2$.

4 CONCLUSIONS

We calculated the overall reaction rate coefficients for the radiative association of $Na^+ + H_2$ and $Na^+ + D_2$ at the Close Coupling level using a recent 3D PES and dipole moment surface. We found that the total number of bound states of $Na^+ - D_2$ is almost three times larger than for $Na^+ - H_2$ due to the mass difference. Similarly, the maximum value of J supporting bound states is larger for the $Na^+ - D_2$ complex, 36, while it is only 26 for $Na^+ - H_2$. These differences result in an overall larger value of the RA rate constant for $Na^+ + D_2$ which reaches a maximum value of approximately $5 \times 10^{-18} cm^3 molecule^{-1} s^{-1}$ at 200 K while the maximum value of the $Na^+ + H_2$ RA rate coefficient, $7 \times 10^{-20} cm^3 molecule^{-1} s^{-1}$ is reached at 100 K.

An interesting result in the present study is that the j=2 rotational states of H_2 and D_2 give notably larger cross sections than the other rotational states.

The reaction rate coefficients obtained in this study are the first Close Coupling RA values obtained for $Na^+ - H_2$ and are closer to the ones predicted by Smith et al. (1983) than

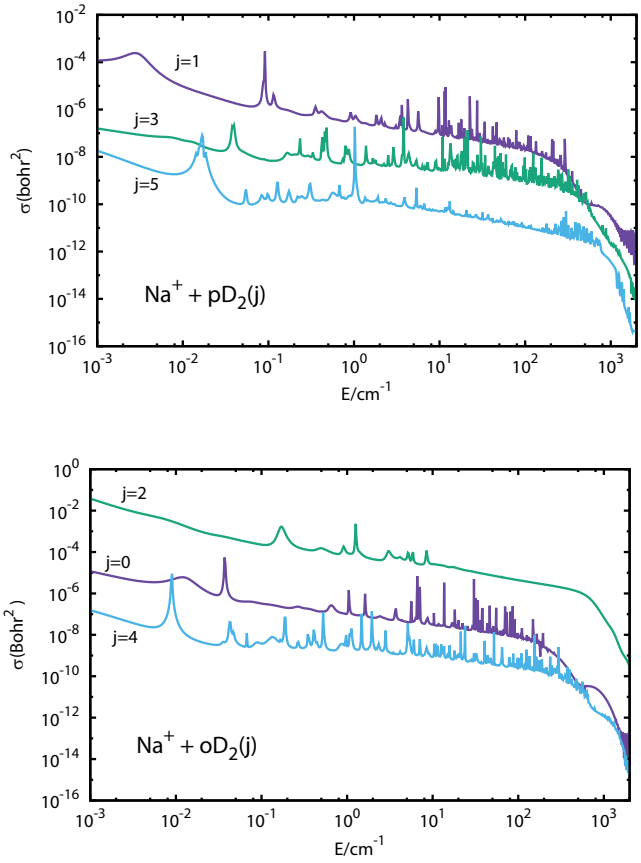

Figure 6. Dependence of the $Na^+ + D_2(v = 0, j)$ RA cross section as a function of rotational excitation illustrated for three values of the rotational quantum number of each of the two spin isomers of D_2 : The upper panel shows the results for the $j = 1, 3, 5$ states of para D_2 while the lower panel shows those for the $j = 0, 2, 4$ states of ortho D_2.

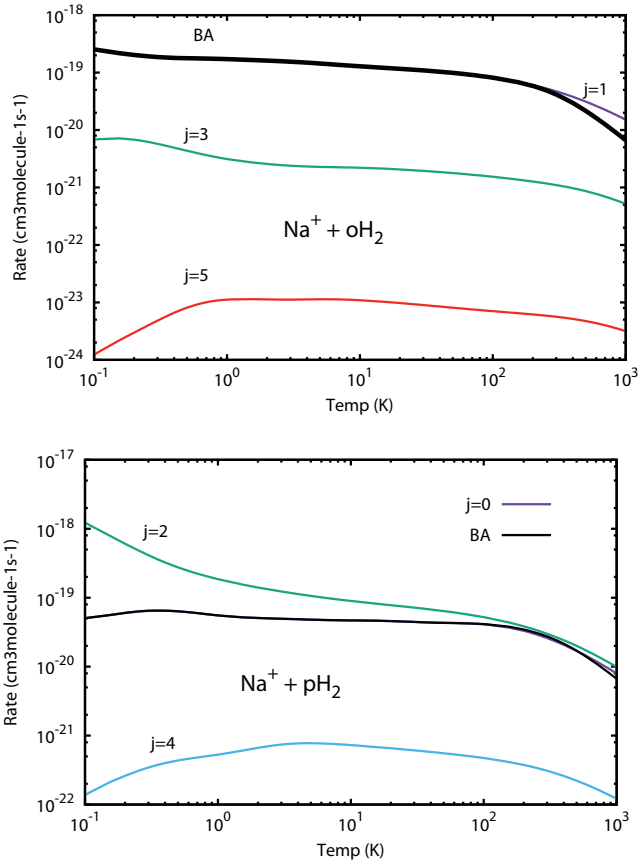

Figure 7. Dependence of the $Na^+ + H_2(v = 0, j)$ RA rate coefficient as a function of rotational excitation illustrated for three values of the rotational quantum number of each of the two spin isomers of H_2 : The upper panel shows the results for the $j = 1, 3, 5$ states of ortho H_2 while the lower panel shows those for the $j = 0, 2, 4$ states of para H_2. In each of these two panels the Boltzmann averaged rate coefficient is also shown for the para and ortho species of H_2

to those of the later study of Petrie & Dunbar (2000). As a matter of fact the present Close Coupling $Na^+ - H_2$ RA value is only 10 times smaller than the one of Smith et al. (1983). We therefore conclude in agreement with these authors that the $Na^+ - H_2$ RA rate coefficients are large enough for this mode of production of NaH in the gaz phase to need to be included in the chemistry models of dense molecular clouds.

5 ACKNOWLEDGMENTS

The authors gratefully acknowledge the support of the COST Action CM1405 entitled MOLIM (Molecules in Motion) for the stay of Daria Burdakova in Bordeaux. Computer time for some of the quantum dynamics computations was provided by the Mesocentre de Calcul Intensif Aquitain computing facilities of the Université de Pau et des Pays de l'Adour.

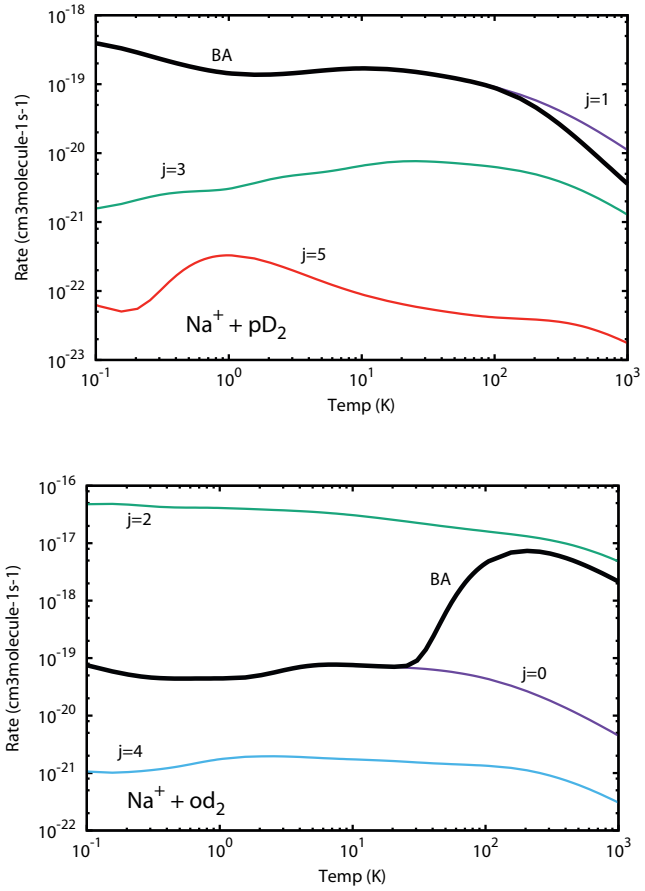

Figure 8. Dependence of the $Na^+ + D_2(v = 0, j)$ RA rate coefficient as a function of rotational excitation illustrated for three values of the rotational quantum number of each of the two spin isomers of D_2 : The upper panel shows the results for the $j = 1, 3, 5$ states of para D_2 while the lower panel shows those for the $j = 0, 2, 4$ states of ortho D_2. On each of these two panels the Boltzman averaged rate coefficient is also shown for the para and ortho species of D_2

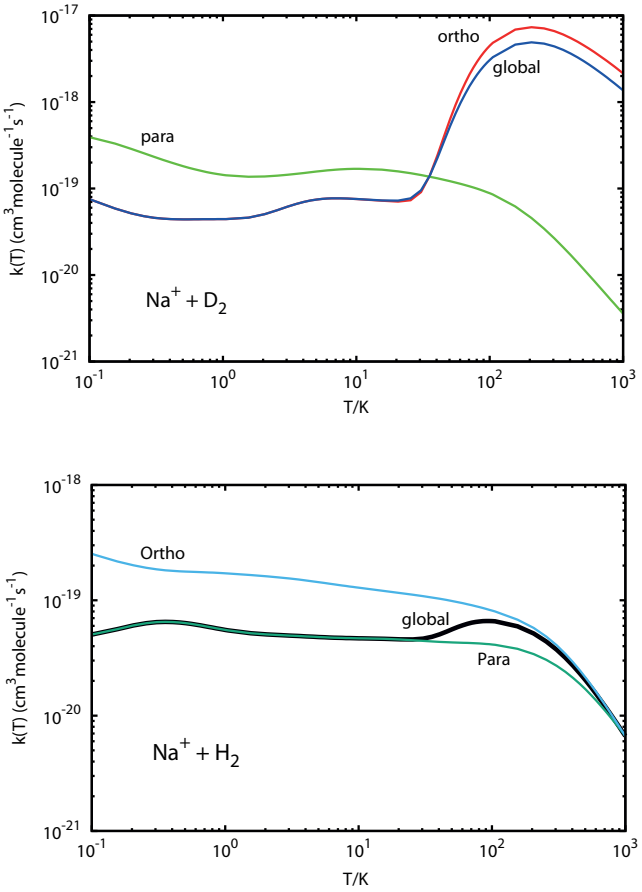

Figure 9. The lower and upper panels of this figure show respectively the temperature dependence of the $Na^+ + H_2$ and $Na^+ + D_2$ RA rate coefficients. For each molecule, the contributions of the two spin isomers are given as well as the result of total Boltzmann averaging.

REFERENCES

Ajili Y., Trabelsi T., Denis-Alpizar O., Stoecklin T., Császár A. G., Mogren Al-Mogren M., Francisco J. S., Hochlaf M., 2016, Phys. Rev. A, 93, 052514
Ayouz M., Lopes R., Raoult M., Dulieu O., Kokoouline V., 2011, Phys. Rev. A, 83, 052712
Balint-Kurti G. G., Shapiro M., 1981, Chem. Phys., 61, 137
Band Y. B., Freed K. F., Kouri D. J., 1981, J. Chem. Phys., 74, 4380
Halvick P., Stoecklin T., Lique F., Hochlaf M., 2011, J. Chem. Phys., 135, 044312
Heather R. W., Light J. C., 1983, J. Chem. Phys., 78, 5513
Hollebeek T., Ho T.-S., Rabitz H., 1999, Ann. Rev. Phys. Chem., 50, 537
Hutson J. M., 1994, Comput. Phys. Comm., 84, 1
Julienne P. S., Krauss M., 1973, Molecule Formation by Inverse Photodissociation. John Wiley and Sons
Lique F., Halvick P., Stoecklin T., Hochalf M., 2012, J. Chem. Phys., 136, 244302
Mrugala F., Spirko V., Kraemer W. P., 2003, J. Chem. Phys., 118, 10547
Munro J. J., Ramanlal J., Tennyson J., 2005, New Journal of Physics, 7, 196
Nyman G., Gustafsson M., Antipov S., 2015, Int.Rev. Phys. Chem., 34, 385
Petrie S., Dunbar R. C., 2000, J. Chem. Phys., 104, 4480
Plambeck R., Erickson N., 1982, Apj, 262, 606
Poad B. L. J., Wearne P. J., Bieske E. J., Buchachenko A. A., Bennett D. I. G., Klos J., Alexander M. H., 2008, J. Chem. Phys., 129, 184306
Poad B. L. J., Dryza V., Klos J., Buchachenko A. A., Bieske E. J., 2011, J. Chem. Phys., 134, 214302
Prasad S. S., Huntress Jr. W. T., 1980, ApJS, 43, 1
Smith D., Adams G., Alge E., herbst E., 1983, Apj, 272, 365
Stoecklin T., Lique F., Hochlaf M., 2013, Phys. Chem. Chem. Phys., 15, 13818
Stoecklin T., Halvick P., Lara-Moreno M. d. J., Trabelsi T., Hochlaf M., 2018a, Faraday Discuss., pp –
Stoecklin T., Halvick P., Yu H.-G., Nyman G., Ellinger Y., 2018b, MNRAS, 475, 2545